Current self-oscillation induced by a transverse magnetic field in a doped GaAs/AlAs superlattice

Baoquan Sun,* Jiannong Wang,† Weikun Ge, and Yuqi Wang
Physics Department, Hong Kong University of Science and Technology, Clear Water Bay, Kowloon, Hong Kong, China

Desheng Jiang, Haijun Zhu, Hailong Wang, Yuanming Deng, and Songlin Feng
NLSM, Institute of Semiconductors, Chinese Academy of Sciences 100083, Beijing, China
(Received 12 February 1999; revised manuscript received 12 April 1999)

We investigate the influence of a transverse magnetic field on the current-voltage characteristics of a doped GaAs/AlAs superlattice at 1.6 K. The current transport regimes—stable electric field domain formation and current selfoscillation—are observed with increasing transverse magnetic field up to 13 T. Magnetic-field-induced redistribution of electron momentum and energy is identified as the mechanism triggering the switching over of one process to another leading to a change in the dependence of the effective electron drift velocity on electric field. Simulation yields excellent agreement with observed results. [S0163-1829(99)00632-3]

Static electric field domains in doped GaAs/AlAs superlattice (SL) were first observed in a transport experiment by Esaki and Chang.[1] The well-defined high- and low-field domains in weakly coupled SL are attributed to the existence of negative differential velocity originated from sequential resonant tunneling between the subbands of the SL. Recently, damped and undamped temporal current selfoscillations under dc bias were observed in SL within a certain range of carrier concentrations.[2–5] The origin of current selfoscillations is an oscillating charge layer accumulated at domain boundary. Above and below this carrier concentration range, the current selfoscillations disappear, and a buildup of stable electric field domains at higher carrier concentrations or a state of uniform electric field distribution at lower carrier concentrations is observed. The variation of carrier concentrations in a SL is achieved experimentally by photoexcitation or doping. The switching between stable field domains and the current self-oscillations can also be obtained by limiting the injected current into a SL.[4] So far, all studies on current self-oscillation are focused on the effect of changing the carrier concentrations in SL. We show that changing the shape of the electron drift velocity-field dependence can also induce current self-oscillations. The shape of the electron drift velocity-field dependence is modified in this experiment by a transverse magnetic field (B); i.e., B is perpendicular to the current direction. By changing B it is possible to tune the tunneling processes from stable field domains to unstable field domains (current self-oscillation) in a SL.

In this paper, the tunneling processes in a doped GaAs/AlAs SL were investigated at 1.6 K in the presence of a transverse B up to 13 T. The sawtoothlike current branch amplitudes in the current-voltage, I(V), characteristics associated with the well-to-well hopping of the stable field domain boundary through the SL decrease with increasing B and disappear at a certain B. Temporal current self-oscillations at a fixed dc bias are then observed. Further increase of B suppresses the temporal current self-oscillations. The observed results are interpreted in terms of the changing dependence of drift velocity on electric field caused by B-induced redistribution of the tunneling electron momentum and energy. Simulations based on a phenomenological model are in excellent agreement with the observed results.

The doped GaAs/AlAs superlattice wafer investigated in this work was grown by molecular-beam epitaxy (MBE) in a VGMKII system. The SL consisting of 40 periods of 14-nm GaAs well and 4-nm AlAs barrier was sandwiched between two n^+-GaAs contacting regions. Only the center 10 nm of the GaAs well was doped with Si($n=2\times10^{17}\,\mathrm{cm}^{-3}$), to insure the interface quality. The wafer was fabricated into mesas with a typical area of 0.01 mm^2. The I(V) characteristics of the devices were measured at 1.6 K in the presence of magnetic fields up to 13 T. The current self-oscillations were recorded with a HP54600A digital oscilloscope.

In this paper, we focus on the second current plateau. Figure 1 shows the measured I(V) curves at various transverse magnetic fields for the second current plateau. In this current plateau at $B=0$, the applied bias for the first negative differential conductance related current peak (2.528 V) corresponds to the homogeneous electric field distribution resulting in the ground state (E_1) to the first excited state (E_2) resonance between neighboring wells. From this field on, the low- and high-electric field domains are formed due to $E_1 \rightarrow E_2$ and $E_1 \rightarrow E_3$ (the second excited state in the well) resonance, respectively.[6] The typical sawtoothlike current

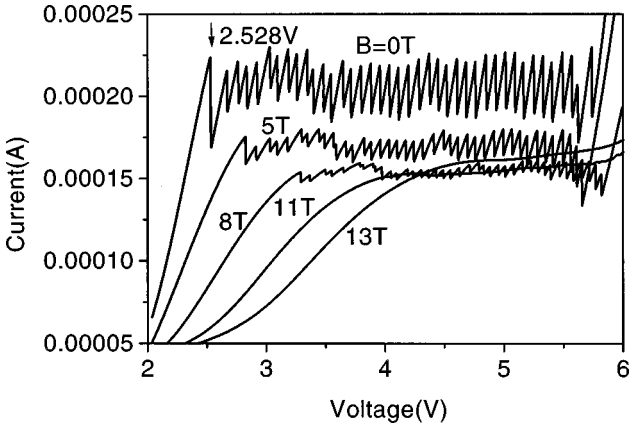

FIG. 1. I(V) curves measured at 1.6 K in the presence of transverse magnetic fields indicated.

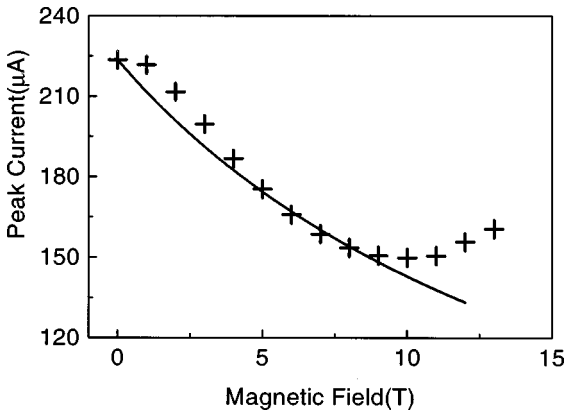

FIG. 2. The solid cross is the measured first peak current as a function of *B*. The solid line is a theoretical fit (see text).

branches in I(V) curves are caused by the electric field domain boundary moving discontinuously through the SL. In this case, there are 40 branches as the same number as the SL period. The measured energy difference between E_1 and E_2 is 63 meV (=2.528 V/40, at $B=0$ T), which is in good agreement with the value of 64 meV calculated by using the Kronig-Penney model. As the transverse magnetic field is increased, the applied bias for the current branches in I-V curve shifts to higher voltage monotonically. The average plateau current, on the other hand, is first decreased with the increase of *B* and then starts to increase with further increase of *B*. The change of the average plateau current with *B* is plotted in Fig. 2, where the first peak current values (cross symbols) are used instead of the average plateau-current values as the two currents change with *B* in the same way. We can see that the peak current is decreased with increasing *B* up to about 9 T and then is increased with further increase of *B*.

In addition, the magnitude of the current branches decreases with increasing *B* and disappears at around 11 T. This is shown more clearly in Fig. 3(a), which is a magnification of the same measurements shown in Fig. 1. As we can see, a current dip extended from 4.03 to 4.32 V (indicated by arrows) appears in the curve with $B=10.5$ T, the dip moves to higher voltage range with increasing *B* and continues up to $B=12.5$ T. Within this dip region, the temporal current oscillations are observed under a fixed dc voltage. Examples of the measured temporal current oscillations at various *B* and *V* are shown in Fig. 3(b). The oscillation frequencies are around 1 MHz.

The monotonic shift of bias to higher voltage with increasing *B* has been reported before and is well understood.[7,8] In brief, if the magnetic-field direction is parallel to the *x* axis and the current flows along *z* axis, an electron that travels the tunneling distance *l* from one well to the next picks up transverse momentum $\hbar k_y = eBl$ due to the Lorentz force. In the effective mass approximation this corresponds to an energy $\Delta E = e^2B^2l^2/(2m^*)$ that is transferred from *z* to *y* direction. Therefore, in order to maintain the resonance condition, this energy transfer has to be compensated by an additional electric field $\Delta F = \Delta E/(el)$.

The current density at the first peak is determined by the resonant tunneling process between the $E_1 \rightarrow E_2$ subbands in the SL. The influence of a transverse *B* on the electronic

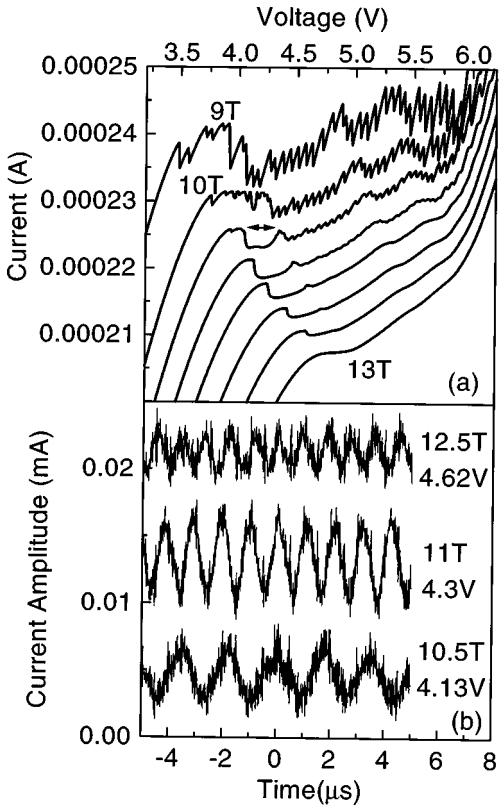

FIG. 3. (a) I(V) curves in the presence of the transverse magnetic fields at 9, 10, 10.5, 11, 11.5, 12, 12.5, and 13 T, respectively from top to bottom. (b) The measured temporal current oscillations at different fixed dc bias and magnetic fields as indicated. The curves in (a) and (b) are offset for clarity.

states of a SL has been given by Mann[9] and a quantum mechanical description of the magnetotunneling through double barriers was performed by Brey, Platero, and Tejedor[10] However, in this paper for simplicity and in the first order of approximation, we propose a simple model based on the calculation by Kazarinov and Suris.[11] Their calculation of a weakly coupled SL at $B=0$ gives the following expression for the dependence of the current density *J* on the electric field *F*

$$J = enl[1-\exp(-\Delta/kT)]\frac{2|\Omega|^2\tau}{1+\varepsilon^2\tau^2}, \tag{1}$$

where $\hbar\epsilon = elF - \Delta$ is the energy detuning from resonance, Δ is the energy separation between subbands, Ω is the matrix element of the Hamiltonian between the ground state of the nth well and the first excited state in the $(n+1)$th well divided by $\hbar$, τ is the relaxation time for the transverse momentum, *n* is the electron density in the wells, and *l* is the SL period. Substituting τ with $\hbar/\Gamma$ in Eq. (1), where Γ is proportional to the width of the current peak in the field dependence of the current density given by Eq. (1), we obtain

$$J = enl[1-\exp(-\Delta/kT)]\frac{2\hbar|\Omega|^2\Gamma}{(eFl-\Delta)^2+\Gamma^2}. \tag{2}$$

The transverse magnetic field causes redistribution of the tunneling electron momentum and energy. In order to con-

serve the momentum and energy in the tunneling process, the resonant peak voltage shifts to a higher value and the width of the resonance peak increases with increasing B. The B-induced additional electric field is given by $\Delta F = eB^2l/(2m^*)$, as discussed above. As the current through the SL is determined by the resonant tunneling process between the $E_1 \rightarrow E_2$ subbands in the adjacent wells the width of the resonance peak, after taking into account the B-induced broadening, can be approximately written as[8]

$$\Gamma(B) = \Gamma(0) + \alpha[2\hbar^2 k_f k_y / m^*], \tag{3}$$

where k_f is the Fermi wave vector of the electron in the nth well, k_y is the B-induced wave-vector shift of the electron tunneling from the nth to the $(n+1)$th well, α equals to $\frac{1}{2}$ for triangular peak and can be used as an adjustment parameter determined by experimental measurement to account for the difference between the shape of a real peak and the triangular one. Adding B-induced additional electric field and peak width broadening into Eq. (2), the electric and magnetic-field dependence of the tunneling current density is then given as

$$J = enl[1 - \exp(-\Delta/kT)] \times \frac{2\hbar|\Omega|^2\Gamma(B)}{(eFl - \Delta - e^2l^2B^2/2m^*)^2 + \Gamma(B)^2}, \tag{4}$$

where the matrix element Ω is taken approximately independent of B.

The solid line in Fig. 2 is the fit using Eq. (4) for $E_1 \rightarrow E_2$ resonance with $\alpha = 0.16$. We can see that the influence of a transverse magnetic field on the electron resonant tunneling process can be well described by Eq. (4) for $B < 10\,\mathrm{T}$. However, for $B > 10\,\mathrm{T}$ the measured peak current deviates from the calculation. The exact origin of this deviation is unclear at the moment.

The current self-oscillations in intrinsic or doped SL have previously reported experimentally and simulated theoretically by only changing the carrier concentrations.[12–15] We show below that changing the shape of the effective electron drift velocity-field dependence can also induce current self-oscillations. We use a discrete model to simulate our result. The model has been successfully used to simulate the effect of carrier concentration on the dynamics of electric field domains in SL. For doped, weakly coupled SL, transport properties in the growth direction can be described by the following equations:[13]

$$\frac{1}{l}(F_i - F_{i-1}) = \frac{e}{\in}(n_i - N_d), \tag{5}$$

$$\in \frac{dF_i}{dt} + en_i\nu(F_i) = J, \tag{6}$$

$$l\sum_{i=1}^{N} F_i = V. \tag{7}$$

Equation (5) is the Poisson equations averaged over one SL period l. Equation (6) is Ampere's law at the ith well establishing that the total current density is the sum of the displacement current and the electron flux due to sequential resonant tunneling. Equation (7) is the voltage bias condition. In these equations, $i = 1,2,\ldots,N$ is the well index, F_i is the average electric field in the ith well, and n_i is the electron concentration in the ith well. ε, N_d, and V are the average permittivity of the SL, the average doping concentration in the well, and the external dc bias, respectively. $\nu(F)$ is the effective electron velocity field dependence, which has maxima at the resonant fields for subbands alignment in neighboring wells. The boundary condition near the contact $\varepsilon(F_1 - F_0)/el = n_1 - N_d = \delta$ allows for a small negative charge accumulation in the first well ($\delta \ll N_d$) to account for the difference of electron density between the contact and SL, which is taken as a fitting parameter varied with magnetic fields. The physical origin of δ is that the n-doped SL is typically sandwiched between two n^+-doped contacting layers thereby forming a n^+-n-n^+ diode.[13] Then some charge will be transferred from the contact to the first well creating a small dipole field that will cancel the electron flow caused by the different concentration of electrons at each side of the first barrier. The initial conditions are $F_i = V/Nl$. Combining Eqs. (5), (6), and (7) and rendering them dimensionless using the characteristic physical quantities, we obtain N dimensionless equations for the electric field distributions

$$\frac{dD_i}{d\tau} = \frac{1}{N}\sum_{j=1}^{N} \nu(D_j)(D_j - D_{j+1} + \gamma) - \nu(D_i)(D_i - D_{i-1} + \gamma) \tag{8}$$

and an expression for the current density

$$J(t) = \frac{\varepsilon F_{1-2}}{Nt_{\mathrm{tun}}}\sum_{j=1}^{N} (D_j - D_{j-1} + \gamma)\nu(D_j), \tag{9}$$

where $D = F/F_{1-2}$ is the dimensionless electric field, $\nu(D) = \nu(F)/\nu(F_{1-2})$ is the normalized and dimensionless effective electron velocity, $\tau = t/t_{\mathrm{tun}}$ where $t_{\mathrm{tun}} = l/\nu(F_{1-2})$ is the characteristic tunneling time, $\gamma = elN_d/\varepsilon F_{1-2}$ is a dimensionless parameter, F_{1-2} is the electric field strength for $E_1 \rightarrow E_2$ resonance peak.

The equations above can be solved numerically by the fourth-order Runge-Kutta method to obtain D_i and $J(t)$. In previous studies,[12–15] the doping concentration was a variable to obtain the condition for the stable or unstable domain formation while the effective electron velocity $\nu(F)$ corresponding to the resonant tunneling current density was an independent function in the simulations. But in our case, the doping concentration is fixed and $\nu(F)$ is the variable. In the presence of transverse magnetic field $\nu(F)$ becomes a function of magnetic field, i.e., $\nu(F,B)$. We assume that $\nu(F,B)$ is proportional to the static tunneling current density $J(F,B)$ given by Eq. (4). Let $\Delta_1 = E_2 - E_1 = 64\,\mathrm{meV}$, $\Delta_2 = E_3 - E_1 = 166\,\mathrm{meV}$, $l = 18\,\mathrm{nm}$, $E_f = 5\,\mathrm{meV}$, $\Gamma = 22\,\mathrm{meV}$, $\alpha = 0.16$, $T = 1.6\,\mathrm{K}$, $m^* = 0.067m_0$, and assuming the width of the peaks has the same B dependence for $E_1 \rightarrow E_2$ and $E_1 \rightarrow E_3$ resonance. The calculated $\nu(F,B)$ are shown in Fig. 4(a) for $B = 0$, 5, and 10 T. γ is related to the doping concentration N_d and the electric field strength F_{1-2}. As $N_d = 2 \times 10^{17}\,\mathrm{cm}^{-3}$ and F_{1-2} shifts to higher voltages with increasing B, as shown in Fig. 4(a), γ is 1.4, 1.25, and 0.96 for 0, 5, and 10 T, respectively. The dimensionless electron drift velocity $\nu(D)$ is shown in the inset of Fig. 4(a), where the solid

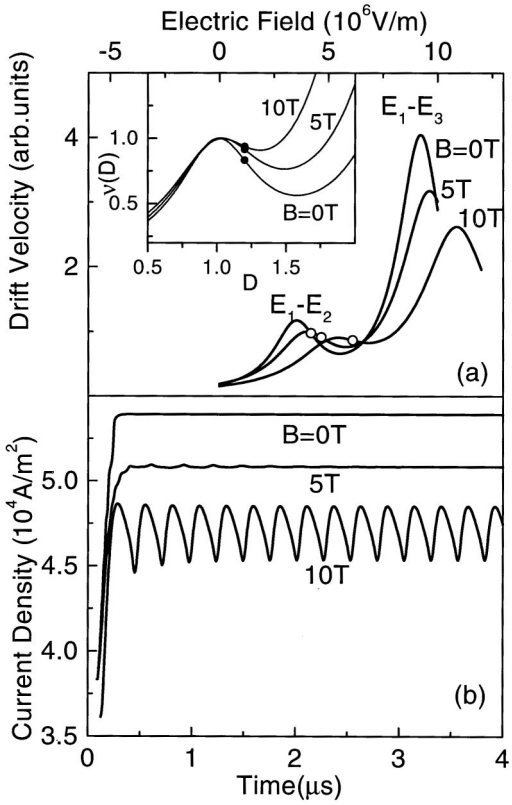

FIG. 4. (a) The calculated drift velocity as a function of electric field with $B=0$, 5, and 10 T, respectively. The open circles indicate the real initial electric field values used in the simulation. The inset shows the dimensionless drift velocity vs dimensionless electric field D with $B=0$, 5, and 10 T, respectively. The solid circles indicate the initial values of D used in the simulation. (b) The calculated current density as a function of time with $B=0$, 5, and 10 T, respectively.

circles indicate the initial values of D $(=1.2)$ used in the simulations for $B=0$, 5, and 10 T. The corresponding real initial electric field values $F_i(0)$ are 3.5, 3.9, and 6.12 $\times 10^6$ V/m, respectively for $B=0$, 5, and 10 T, as indicated by the open circles in Fig. 4(a). The other parameters used in the simulations are as follows: the number of SL period $N=40$, SL period $l=18$ nm, tunneling time $t_{\rm tun}=10$ ns, the boundary condition $\delta'=10^{-3}\gamma$.

The calculated current density $J(t)$ and the electric field distribution through SL region D_i are shown in Figs. 4(b) and 5 for $B=0$, 5, and 10 T, respectively. For $B=0$ and 5 T, constant currents are obtained corresponding to stable high- and low-field domain formation, although there is a small damping wave when time is less than 2 μs at 5 T. The domain boundary is rather sharp and confined roughly with one well. For $B=10$ T, however, temporal current selfoscillations is developed. The domain boundary is less sharp in comparison with that for $B=0$ and 5 T and is extended within several wells. These simulated results are in an excellent agreement with the observed switching from stable to unstable domain formation in our experiment.

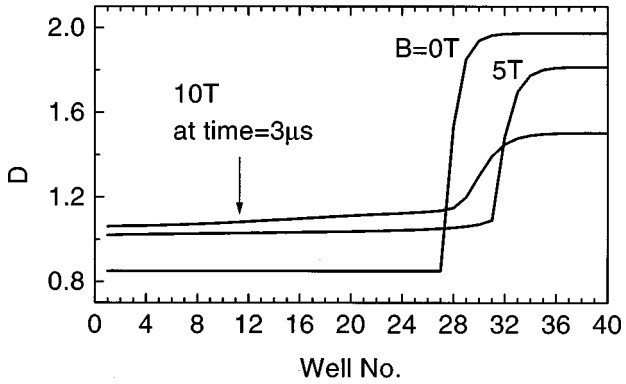

FIG. 5. The calculated distribution of dimensionless electric field through the superlattice region with real initial electric field taken as 3.5, 3.9, and 6.12×10^6 V/m, respectively for $B=0$, 5, and 10 T.

In conclusion, we have investigated the influence of a transverse magnetic field on the tunneling processes in a doped SL. With increasing B, the tunneling processes are switched from the stable to unstable field domain formation. The observations are explained based on the B-induced redistribution of the tunneling electron momentum and energy, which results in the change of the dependence of the effective electron velocity on electric field. The simulated results show that the electric field domain formation is directly related to the dependence of the effective electron velocity on electric field. The simulation and experiment are in excellent agreement.

B. Q. Sun and J. Wang would like to acknowledge the financial support of the Research Grant Council of Hong Kong, China.

*On leave from NLSM, Institute of Semiconductors, Chinese Academy of Sciences, Beijing, China.

†Author to whom correspondence should be addressed. Electronic address: phjwang@ust.hk

[1] L. Esaki and L. L. Chang, Phys. Rev. Lett. **33**, 495 (1974).

[2] R. Merlin, S. H. Kwok, T. B. Norris, H. T. Grahn, K. Ploog, L. L. Bonilla, J. Galan, J. A. Cuesta, F. C. Martinez, and J. Moleara, in *Proceedings of the 22nd International Conference on the Physics of Semiconductors*, edited by D. J. Lockwood (Singapore, World Scientific, 1995) p. 1039.

[3] H. T. Grahn, J. Kastrup, K. Ploog, L. L. Bonilla, J. Galan, M. Kindelan, and M. Moscoso, Jpn. J. Appl. Phys., Part 1 **34**, 4526 (1995).

[4] Baoquan Sun, Desheng Jiang, and Xiaojie Wang, Semicond. Sci. Technol. **12**, 401 (1997).

[5] J. Kastrup, R. Hey, K. H. Ploog, H. T. Grahn, L. L. Bonilla, M. Kindelan, M. Moscoso, A. Wacker, and J. Galan, Phys. Rev. B **55**, 2476 (1997).

[6] For the studied sample, the electric field strength of realizing E_3-E_1 resonance, $F=(E_3-E_1)/el=166/el$, is smaller than that of realizing E_x-E_1 resonance, $F_x=2(E_x-E_1)/el=278/el$, when the lowest $\Delta E_{\Gamma X}\sim160$ meV is considered.

[7] S. Ben Amor, K. P. Martin, J. J. L. Rascol, R. J. Higgins, A. Torabi, H. M. Harris, and C. J. Summers, Appl. Phys. Lett. **53**, 2540 (1988).

[8] S. Ben Amor, J. J. L. Rascol, K. P. Martin, R. J. Higgins, R. C.

Doher, and H. Hier, Phys. Rev. B **41**, 7860 (1990).
[9] J. C. Maan, Festkorperprobleme **27**, 137 (1987).
[10] L. Brey, G. Platero, and C. Tejedor, Phys. Rev. B **38**, 9649 (1988).
[11] R. F. Kazarinov and R. A. Suris, Fiz. Tekh. Polulprovdn. **6**, 148 (1972) [Sov. Phys. Semicond. **6**, 120 (1972)].
[12] L. L. Bonilla, J. Galan, J. A. Cuesta, F. C. Martinez, and J. M. Molera, Phys. Rev. B **50**, 8644 (1994).
[13] O. M. Bulashenko and L. L. Bonilla, Phys. Rev. B **52**, 7849 (1995).
[14] R. Aguado, G. Platero, M. Moscoso, and L. L. Bonilla, Phys. Rev. B **55**, R16 053 (1997).
[15] A. Wacker, M. Moscoso, M. Kindelan, and L. L. Bonilla, Phys. Rev. B **55**, 2466 (1997).